Chapter 4

Microstructure and mechanical behaviour of Fe-30Mn-9Al-0.8C and Fe-20Mn-10Al-1C low-density steels

4.1 Introduction

For large deformation processes such as cold rolling or cold forging, Fe-Mn-Al-C based low-density steel must possess high ductility to allow for multiple deformation passes. A higher amount of austenite results in greater ductility, while a higher amount of ferrite results in reduced ductility. Additionally, ductility is influenced by grain size and the role of precipitates during deformation. Therefore, to retain a higher amount of the austenite phase, selecting a composition that stabilizes austenite during heat treatment and optimizing the heat treatment sequence becomes crucial. The aim of this chapter is to provide the information related to the production of high ductility material using the selected compositions: (a) Fe-30Mn-9Al-0.9C (S1) and (b) Fe-20Mn-10Al-1C (S2) low-density steels. Additionally, it aims to study the microstructural and mechanical behavior of these materials. The steels are produced using a vacuum induction melting furnace, following the procedure outlined in Section 3.2.1 of Chapter 3. The schematics of the thermo-mechanical processing applied to the steels are shown in Fig. 9 of Chapter 3. Microstructure, phase composition, and their quantification are analyzed using optical microscopy and X-ray diffraction. The mechanical properties are evaluated through tensile testing and hardness measurement.

4.2 Results and discussion

4.2.1 Material alloying compositions

The chemical analysis of the solutionised and WQ steels are given in Table 7. The alloy SS1 contains Fe-30.6%Mn-9.1%Al-0.79%C-0.15%Si-0.01%P-0.02%S (all by mass %).

The alloy SS2 contains Fe-20.1%Mn-10.2%Al-1.01%C-0.15%Si-0.01%P-0.02%S (all by mass %).

Table 7: Chemical composition of SS1 and SS2 low-density steels.

Alloy	Mn	Al	C	Si	Cr	Ni	Fe
SS1	30.6	9.1	0.79	0.15	0.01	0.02	Bal.
SS2	20.1	10.2	1.01	0.15	0.01	0.02	Bal.

4.2.2 Microstructural analysis

The optical microstructure of FS1 and SS1 steels is shown in Fig. 18a and 18b respectively. Hot forging has been conducted between 1200°C and 900°C with the specific objective of breaking the dendritic structure through substantial plastic deformation exceeding 60%. The processes of solutionisation and WQ are commonly employed in metallurgy to achieve desired material properties. In these micrographs, austenite appears grey, ferrite appears white, and porosity is represented in black.

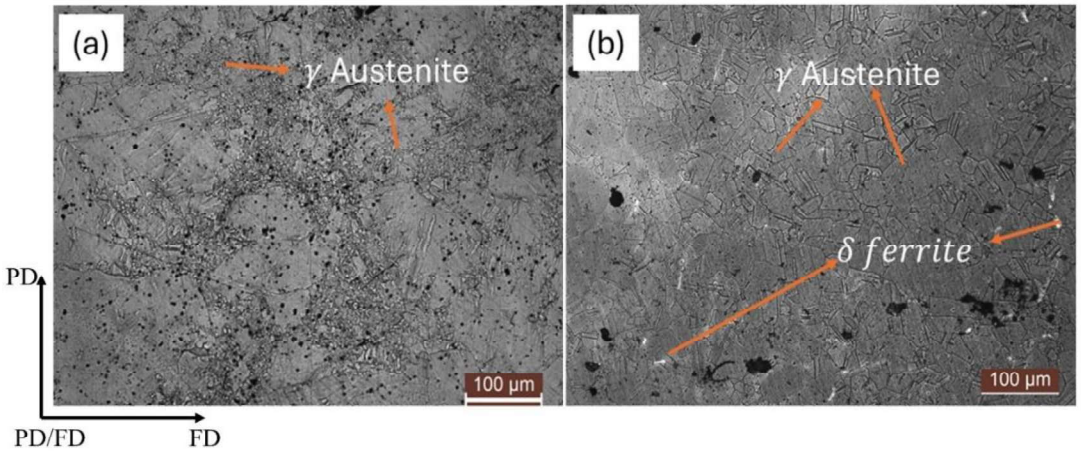

Fig. 18: OM of S1 steel (a) hot forged & WQ, (b) solutionised & WQ.

Figure 18a predominantly displays the grey color, indicating a fully austenitic phase after hot forging. However, there is segregation of very fine austenite grains across the surface, which may be due to non-uniform strain distribution during biaxial hot forging. In highly

strained regions, the rate of dynamic recrystallization is higher compared to less strained regions. After hot forging, the workpiece is WQ, resulting in the retention of the austenitic structure which is mainly because the manganese element is austenite stable phase. The microstructure ranges from very fine austenitic grains, including those smaller than 10 µm, to coarse grains up to 150 µm in size. Figure 18b shows a uniform austenite matrix with annealing twins present in most grains. The average grain size is 50 µm. Solutionisation at 1050°C reduces and homogenizes the strained regions, and WQ results in a uniform austenite structure. However, very small white ferrite regions can still be observed within the austenite matrix.

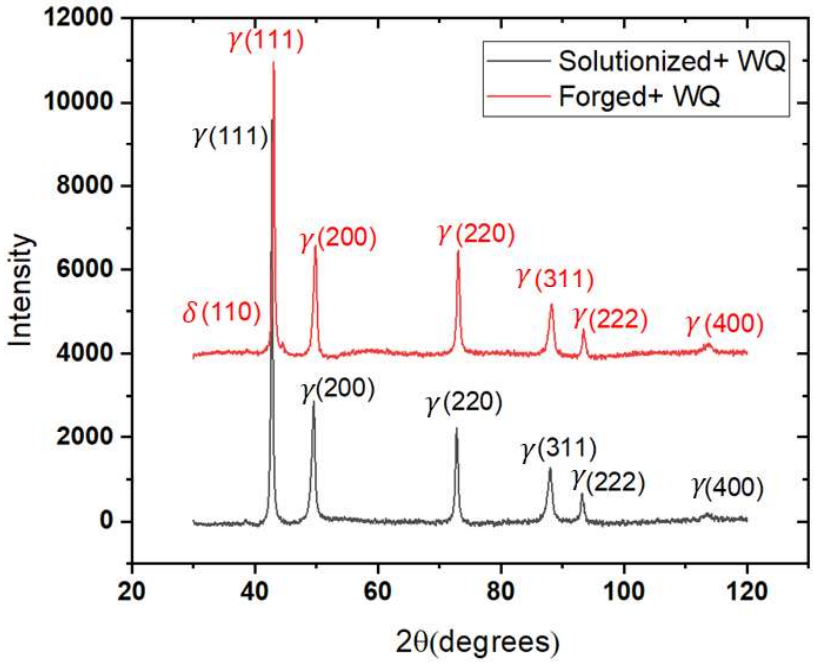

Fig. 19: XRD pattern of S1 steel.

According to the XRD profile (Fig. 19), the diffraction peaks corresponding to FCC γ-austenite and BCC δ-ferrite are clearly identified. It can be confirmed that the hot-forged steel is primarily composed of austenite (98.5%) with a small amount of ferrite (1.5%).

However, after solutionisation at 1050°C and WQ, a fully austenitic phase is achieved. Therefore, SS1 is an austenitic low-density steel.

Figures 20a and 20b show the optical microstructure of FS2 and SS2 respectively. In Fig. 20a, two phases are visible: ferrite, appearing as isolated white islands some of which are elongated and some are round in shape, embedded within the austenite matrix. Also, there is segregation of austenite grains due to varying rates of dynamic recrystallization during biaxial hot forging. Aluminium acts as a ferrite stabilizer, so the higher aluminium content leads to ferrite formation during quenching.

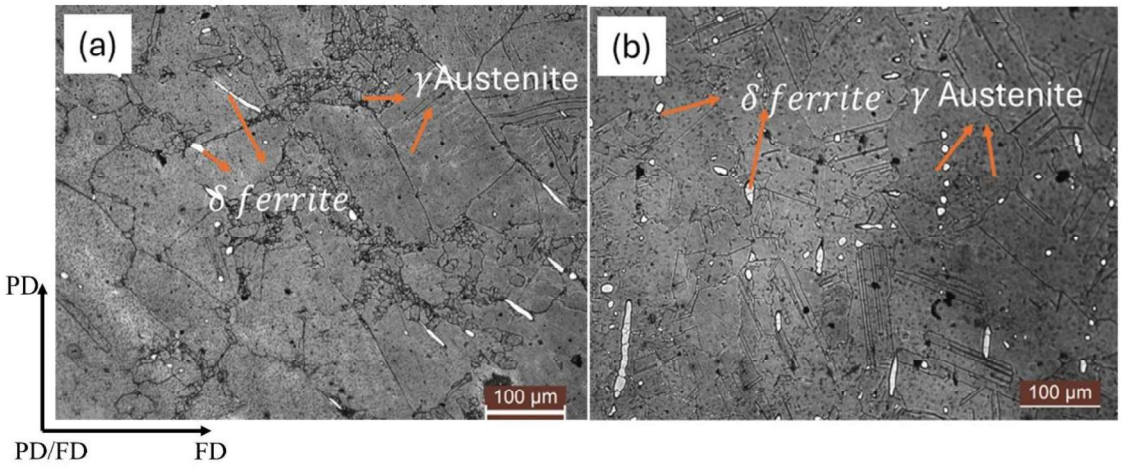

Fig. 20: OM of S2 steel (a) forged, WQ, (b) solutionised at 1050°C, WQ.

After solutionisation and WQ, the segregations are dissolved, resulting in the formation of equiaxed austenite. Ferrite is evenly distributed along the austenite boundaries; however, the amount of ferrite is increased compared to the biaxial hot forging process. The average grain size of the austenite is approximately 80 µm, while the ferrite grain size is around 10 µm. Some of the elongated ferrite structures have broken into a round shape.

According to the XRD profile (Fig. 21), it can be confirmed that the hot-forged steel is predominantly composed of austenite, which differs from the optical image. However, after solutionisation and WQ, the diffraction peaks corresponding to FCC γ-austenite and BCC

δ-ferrite are clearly identified. This confirms that the fraction of ferrite increases after solutionisation and WQ. The SS2 steel has austenitic microstructure with 5% ferritic microstructure and called as duplex steel.

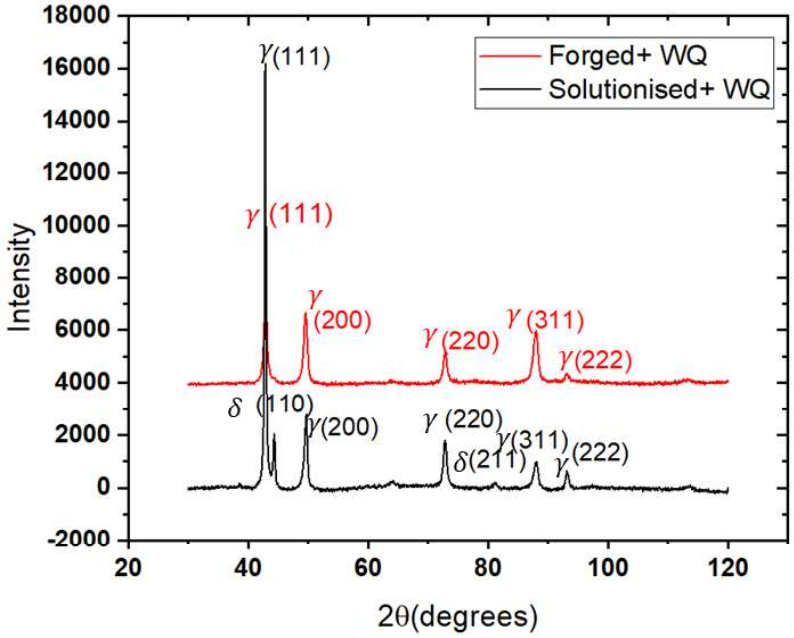

Fig. 21: XRD pattern of S2.

4.2.3 Tensile properties

The engineering stress-strain curves for FS1 steel and SS1 steel samples are displayed in Fig. 22a, and their tensile properties are summarized in Table 8. According to the data in Table 8, the FS1 steel has an ultimate tensile strength of 868 MPa, a yield strength of 580 MPa, and a total elongation of 30%. The presence of segregated austenitic structures in the hot-forged steel may contribute to anisotropy in its mechanical properties. The engineering stress-strain curve of the SS1 steel, shown in Fig. 22a, exhibits continuous strain hardening during tensile testing at room temperature. The yield strength and ultimate tensile strength of the sample are 380 MPa and 762 MPa, respectively.

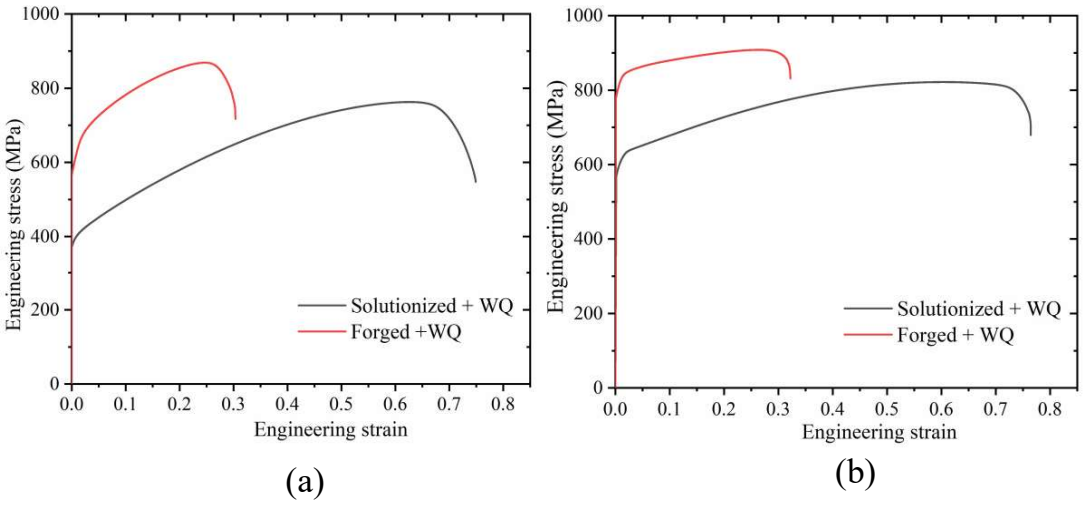

Fig. 22: Stress-strain curve of (a) S1, (b) S2 steels.

Table 8: Tensile properties.

Sample	YS (MPa)	UTS (MPa)	TE (%)	UE (%)
FS1	580±30	868±60	30±2.9	25±2.7
SS1	380±12	762±19	74.8±1.8	64±1.5
FS2	785±38	908±81	30±2.4	25±2.1
SS2	570±15	821±23	76.4±1.9	60±0.7

The SS1 sample achieved a high elongation to fracture of 74.8 %, which is the percentage ratio of total deformation of the gauge length after tensile fracture to the original gauge length. Compared to FS1, the ultimate tensile strength and yield strength decreased by 0.89 times and 0.65 times, respectively, while the elongation increased by a factor of three. The strength and total elongation are slightly lower than those of fully austenitic Fe–Mn–Al–C steel, likely due to the presence of BCC ferrite in the austenite matrix [84]. The PSE = (UTS × TE) values for the SS1 steel is 57 GPa %, which is lower than the 67.7–84.6 GPa·% range observed in the Fe-28Mn-9Al-0.8C alloy fabricated by cold rolling and heat treatment, as studied by Yoo et al. This difference is likely due to the larger austenitic grain

size in the present alloy, approximately 50 μm, compared to the 5–38 μm grain size in the Fe-28Mn-9Al-0.8C alloy, as reported by Yoo et. Al [84].

Engineering stress-strain curves for FS2 and SS2 steel are shown in Fig. 22b. At room temperature, the FS2 exhibits a yield strength of 785 MPa, an ultimate tensile strength of 908 MPa, and a total elongation of 46%. The specific strength (SS = UTS/density) reaches 139.6 MPa.cm³/g, which is higher than that reported for similar compositions in the literature [51]. Despite its excellent specific strength, the FS2 steel has non-uniform mechanical properties, as indicated by the large standard deviation in the obtained values. This variation is attributed to the non-uniform grain sizes in the microstructure. After solution treatment, the tensile strength decreases while the elongation significantly improves. At room temperature, the SS2 exhibits an yield strength of 570 MPa, an ultimate tensile strength of 821 MPa, and a total elongation of 76.4%. The PSE value of the solution-treated steel reaches 62.3 GPa %, which is 129% higher than that of the FS2 steel. This improvement in ductility can be attributed to the separation of banded-structure δ-ferrite grains and stress relaxation.

According to the XRD profile (Fig. 21), it can be confirmed that the FS2 and SS2 steels are basically composed of austenite and ferrite. The ferrite phase is δ-ferrite phase. Zhang et al. [167] confirmed the formation of numerous mobile dislocations in ferrite. This phenomenon occurs because austenite has a higher thermal expansion coefficient and smaller specific volume compared to ferrite. During rapid cooling via water quenching, austenite grains experience significant volume contraction, leading to tensile stress and the formation of randomly distributed dislocations in the neighboring, softer ferrite grains [168]. It is illustrated that solution temperature plays significant role in the improvement of mechanical properties of the hot-forged steel.

The PSE for commercial Fe–Mn–Al–C low-density steel is typically between 11 GPa% and 88 GPa%. In the current study, the PSE value reached 57 GPa % for fully austenitic steel and 62.3 GPa % for duplex steel, which are significantly higher than those of TRIP steel, TWIP steel, and traditional Fe–Mn–Al–C low-density steel. The balance between high ultimate tensile strength (762 MPa) and good ductility (74.8%) for austenitic steel, and ultimate tensile strength (821 MPa) and good ductility (76.4%) for duplex steel, meets the production and application requirements for automotive steel. This steel achieves a desirable balance between ultimate tensile strength and ductility, satisfying the demands for high-performance automotive applications.

4.2.4 Hardness

The average hardness of the FS1 steel is found to be 220 ± 30 HV (Fig. 23). After solutionisation and WQ, the average micro-hardness of the S1 is 200 ± 10 HV. For S2, the average hardness of the biaxial hot forged and WQ is 260 ± 30 HV (Fig. 23). After solutionisation and WQ, the average micro-hardness of S2 steel is 230 ± 10 HV.

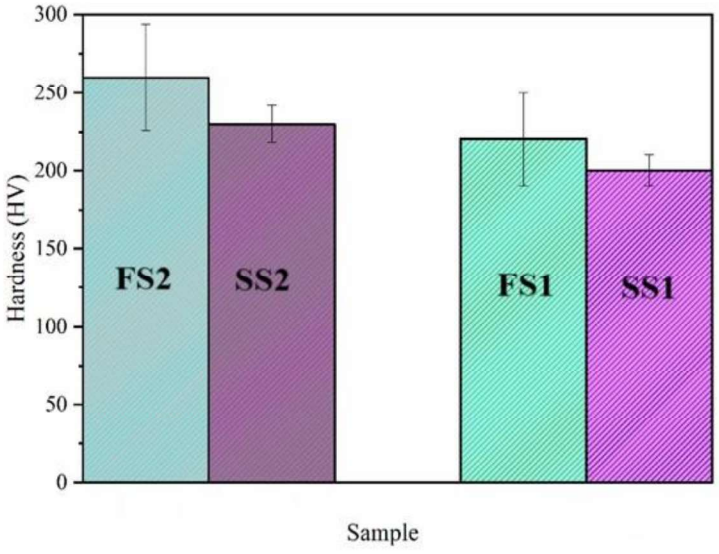

Fig. 23: Hardness value after hot forged & WQ and after solutionisation &WQ for S1 and S2 steels.

The deviation in hardness data at the surface of the forged sample is higher due to the microstructure being composed of both coarse and very fine grain boundaries. The hardness measured in fine grain regions is greater compared to coarse grain regions. The hardness in SS2 is greater than that in SS1 despite the grains being coarser. This may be attributed to the higher number of twins in SS2 compared to SS1.

4.2.5 Fractography

Fractographic observations are also considered to investigate the origins of ductility changes during the hot forging and WQ and during the solutionisation and WQ processes. As shown in Fig. 24, both the fracture surfaces of the FS1 and SS1 samples exhibit dimples signifying the characteristic of ductile fracture. However, significant differences are observed between the fracture morphologies of the FS1 and SS1 sample. The dimples on the fracture surface of the FS1 sample vary in size and are distributed non-uniformly compared to the more uniformly distributed dimples on the SS1 sample. The SS1 sample exhibits reduced strength, plasticity, and strain hardening rate. This reduction is attributed to the uniform distribution of austenite grains formed by the decomposition of segregated grain boundaries into larger austenite grain boundaries during solution treatment. The typical dimple size is a few micrometers, which is smaller than the austenite grain size, indicating that the dimpled areas represent ductile transgranular fracture of austenite.

The fracture surface of FS2 sample displays a mixed fracture mode, characterized by both dimpled and quasi- cleavage areas. In contrast, the fracture surface of the SS1 sample exhibits uniform dimples. Additionally, the dimples in the SS1 sample are larger compared to those in the F1 sample. The FS1 and FS2 steels demonstrated high strength, but lower ductility compared to the SS1 and SS2 steels respectivly. During tensile deformation, microcracks are likely to form along the δ/γ grain boundaries due to the plasticity mismatch

between the banded δ-ferrite and the austenite matrix, eventually leading to macroscopic fractures. As observed in duplex stainless steels, the toughness is affected by the elongated δ distribution in the deformed state.

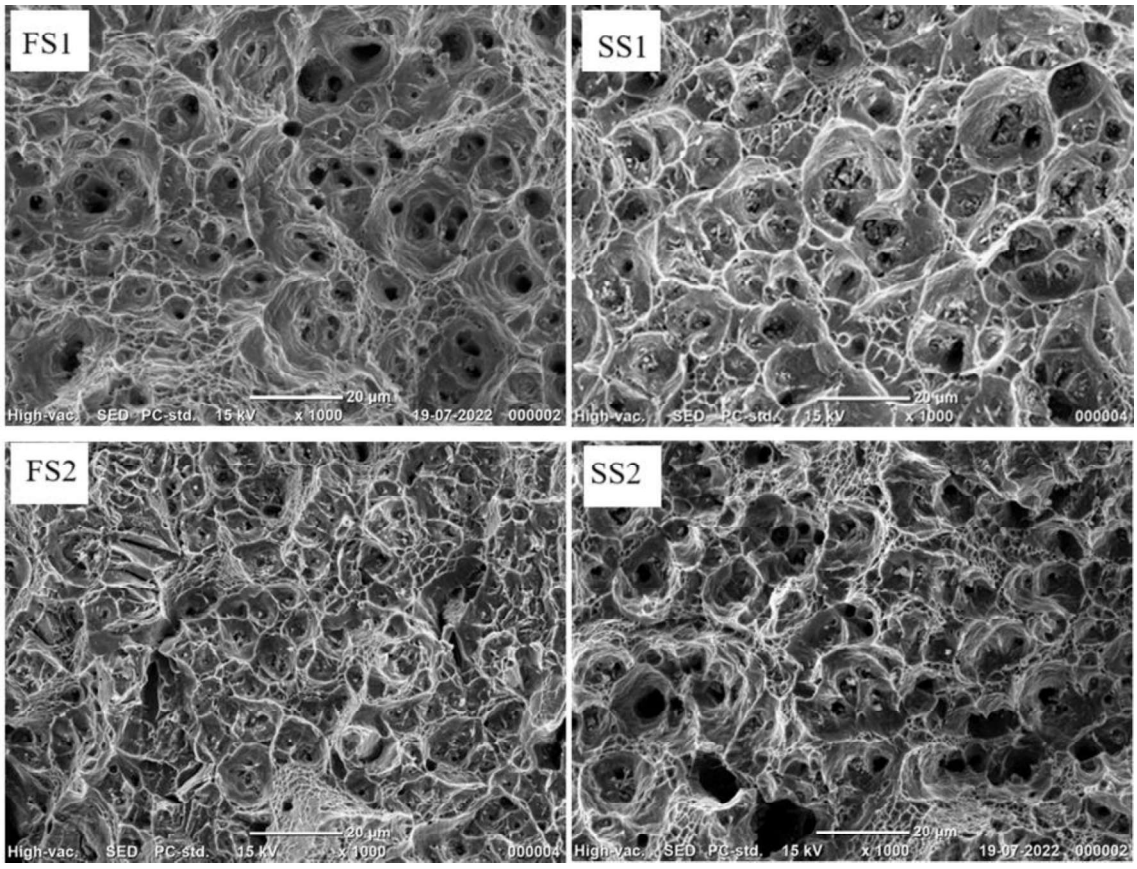

Fig. 24: Fracture morphology after hot forged & WQ and after solutionisation &WQ for S1 and S2 steels.

Following solution treatment at 1050°C for 1 hour, both the steels exhibited a dimpled fracture morphology without any cleavage facets. The average dimple size is measured about 15.8 µm, with numerous deep dimples visible on the fracture surface, indicating enhanced ductility after the treatment.

Both S1 and S2 steels demonstrate good plasticity after solutionisation and WQ. The fracture surfaces of the tensile samples from both alloys reveal numerous micropores at the fracture centers, along with a variety of dimples differing in shape, size, and depth. These features are characteristic of ductile fracture. The presence of large dimples suggests that a significant amount of energy is absorbed during fracture. Generally, larger dimple sizes correlate with increased ductility and toughness in steel.

4.3 Conclusions

The mechanical properties and microstructure of S1 and S2 low-density steels have been investigated. The results obtained are as follows.

1. After solutionisation and WQ, S1 has more than 98.5% austenitic microstructure and it is called as austenitic low-density steel while S2 has austenitic with 5% ferritic microstructure and called as duplex steel.
2. The selected compositions achieve high total elongation greater than 70%. However austenitic one has higher uniform elongation.
3. The yield strength of SS2 steel is 1.5 times greater than that of SS1 steel due to presence of ferrite in prior one.
4. For the hot-forged steel, varying dimple sizes result in a distinctive fracture morphology. After solution treatment at 1000°C for 0.5 hours followed by WQ, the steels exhibit obvious ductile fracture characterized by many deep dimples.